Eur. Phys. J. C (2013) 73:2276
DOI 10.1140/epjc/s10052-013-2276-2

THE EUROPEAN PHYSICAL JOURNAL C

Regular Article - Experimental Physics

On the potentiality of the $ZnWO_4$ anisotropic detectors to measure the directionality of Dark Matter

F. Cappella[1], R. Bernabei[2,3,a], P. Belli[3], V. Caracciolo[4], R. Cerulli[4], F.A. Danevich[5], A. d'Angelo[1,6], A. Di Marco[2,3], A. Incicchitti[6], D.V. Poda[5], V.I. Tretyak[5]

[1]Dip. di Fisica, Università di Roma "La Sapienza", 00185 Rome, Italy
[2]Dip. di Fisica, Università di Roma "Tor Vergata", 00133 Rome, Italy
[3]Sez. Roma "Tor Vergata", INFN, 00133 Rome, Italy
[4]Laboratori Nazionali del Gran Sasso, INFN, 67100 Assergi, Italy
[5]Institute for Nuclear Research, MSP, 03680 Kyiv, Ukraine
[6]Sez. Roma, INFN, 00185 Rome, Italy

Received: 28 September 2012 / Revised: 13 December 2012

Abstract In the anisotropic scintillators the light output and the pulse shape for heavy particles (p, α, nuclear recoils) depend on the direction with respect to the crystal axes; the response to γ/β radiation is isotropic instead. This feature offers the possibility to study the directionality approach, which is applicable in the particular case of those Dark Matter candidate particles inducing just nuclear recoils. Among the anisotropic scintillators, the $ZnWO_4$ has unique features, which make it an excellent candidate for this type of research, and there is still plenty of room for the improvement of its performances. In this paper the possibility of a low background pioneer experiment (named ADAMO—Anisotropic detectors for DArk Matter Observation) to exploit deep underground the directionality approach by using anisotropic $ZnWO_4$ scintillators is discussed.

1 Introduction

Astrophysical observations have given evidence for the presence of Dark Matter (DM) on all astrophysical scales and many arguments have also suggested that a large fraction of the DM should be in form of relic particles. In the direct search for DM, a positive model independent result has been obtained at about 9σ C.L. for the presence of DM particles in the galactic halo by the DAMA/NaI and DAMA/LIBRA experiments [1–3] exploiting the DM annual modulation signature [4, 5] in highly radio-pure NaI(Tl) target over 13 annual cycles. All the many peculiarities of this signature are satisfied by the experimental data; no systematics or side processes able to simultaneously satisfy all the many peculiarities of the DM annual modulation signature and to account for the whole measured modulation amplitude is available (see Refs. [1–3, 6, 7] and references therein). It is worth noting that no other experiment exists, whose result can be directly compared in a model independent way with those by DAMA/NaI and DAMA/LIBRA. Therefore, the model-dependent upper bounds claimed, under a single set of largely arbitrary assumptions, by some activities [8, 9] are not in any robust contrast with DAMA results, also considering that many uncertainties in the procedures they apply in the data handling/reduction exist (see e.g. [1, 10–14]) as well as in many astrophysical, nuclear and particle physics related aspects. The claimed exclusion limits are even more uncertain in the DM particle low mass region, that the pioneer experiment, proposed in this paper, can explore by its distinctive features with an original approach. For completeness, we also remind that recently possible positive hints—exploiting different target materials and approaches, and using modest exposures—have been presented by CoGeNT [15] and CRESST [16].

It is worth noting that the DAMA model independent evidence is compatible with a wide set of scenarios regarding the nature of the DM candidate and related astrophysical, nuclear and particle physics; for example, some given scenarios and parameters are discussed e.g. in Refs. [1, 7, 17–30] and in Appendix A of Ref. [2]. Further large literature is available on the topics [31–72]. In particular, the used approach and target assure sensitivity both to DM candidate particles inducing nuclear recoils as well as to DM candidate particles giving rise to electromagnetic radiation.

[a] e-mail: rita.bernabei@roma2.infn.it

Published online: 17 January 2013

A different possible approach is the directionality [73], in principle effective just for those DM candidate particles able to induce nuclear recoils. This approach studies the correlation between the arrival direction of the DM particles, through the induced nuclear recoils, and the Earth motion in the galactic rest frame. In fact, the dynamics of the rotation of the Milky Way galactic disc through the halo of DM causes the Earth to experience a wind of DM particles apparently flowing along a direction opposite to that of solar motion relative to the DM halo. However, because of the Earth's rotation around its axis, their average direction with respect to an observer fixed on the Earth changes during the sidereal day. The possible nuclear recoils induced by the DM particles are expected to be strongly correlated with their impinging direction, while the background events are not; therefore, the study of the nuclear recoils direction can offer a way for pointing out the presence of the considered DM candidate particles in a way largely independent on the assumptions.

In Sect. 2 we analyze possible experimental techniques to measure the direction of nuclear recoils produced by the DM candidate particles considered here. In particular, anisotropic scintillators are considered as promising detectors sensitive to the recoils direction because of the dependences of their scintillation properties (quenching and scintillation decay kinetics) on the direction of the heavy particles relatively to the crystal axes. In Sect. 3 the zinc tungstate ($ZnWO_4$) anisotropic crystal scintillator is proposed as a promising choice to build a directionality sensitive set-up. Finally, the ADAMO project, based on the use of $ZnWO_4$ crystal scintillators, is presented in Sect. 4, and an example of the reachable sensitivity for a given model is discussed in Sect. 5.

2 Directionality sensitive detectors

In principle low pressure Time Projection Chamber (TPCs), where the range of recoiling nuclei is of the order of mm (while in solid detectors the range of recoiling nuclei is typically of order of μm) might be suitable to investigate this directionality (see e.g. [74, 75]) through the detection of the tracks' directions. However, a realistic experiment with low pressure TPCs can be limited e.g. by the necessity of an extreme operational stability, of an extremely large detector size and of a great spatial resolution in order to reach a significant sensitivity. These practical limitations, affecting possible experiments aiming to measure recoil tracks, can be overcome by using the anisotropic scintillation detectors in a suitable low background experimental set-up located deep underground. In this case there is no necessity of a track detection and recognition, since the information on the presence of candidate particles is given by the variation of the measured counting rate (see later) during the sidereal day when the light output and the pulse shape vary depending on the direction of the impinging particles with respect to the crystal axes.

The use of anisotropic scintillators to study the directionality signature was proposed for the first time in Ref. [76] and revisited in [77],[1] where the case of anthracene detector was preliminarily analysed and several practical difficulties in the feasibility of such an experiment were underlined. Nevertheless, the authors suggested that competitive sensitivities could be reached with new devoted R&D's for the development of anisotropic scintillators having significantly larger size, higher light response, better stiffness, higher atomic weights and anisotropy features similar as—or better than—those of the anthracene scintillator.

Recently, measurements and R&D works have shown that the $ZnWO_4$ scintillators can offer suitable features: they have already a very good radio-purity [80], and an energy threshold at level of few keV is reachable [81]; in addition, there is room for further improvement of their performances. Thus, the $ZnWO_4$ can be an excellent candidate for this type of research due to its unique features. In fact, not only the light output of heavy particles (p, α, nuclear recoils) depends on the direction of such particles with respect to the crystal axes while the response to γ/β radiation is isotropic, but also the scintillation decay time shows this property. Such an anisotropic effect has been ascribed to preferred directions of the excitons' propagation in the crystal lattice affecting the dynamics of the scintillation mechanism [82–89]. Both the anisotropic features of the $ZnWO_4$ detectors can provide two independent ways to exploit the directionality approach. In particular, the presence of heavy ionizing particles with a preferred direction (like recoil nuclei induced by the DM candidates considered here) could be discriminated from the electromagnetic background by comparing the low energy distributions measured by using different orientations of the crystal axes along the day [76, 77]. Moreover, the directionality technique can also be explored at some extent studying the shape of the induced nuclear recoil pulses, as described in the following.

In both cases, a crucial role in the directionality approach is played by the detector velocity in the galactic rest frame, $\vec{v}_d(t)$, which varies with time. It is possible to define $\vec{v}_d(t)$ considering various coordinate frames; in particular, in an horizontal coordinate frame located at the North pole, described by the "polar-zenith", $\theta_z(t)$, and by the "polar-azimuth", $\varphi_a(t)$, the area described in the sky by the direction of $\vec{v}_d(t)$ is only a strip. This is well demonstrated by Fig. 1(left), that shows the possible directions in the sky (identified by the polar and azimuth angles θ_z and φ_a) of

[1] Some preliminary activities have also been carried out by various authors [78, 79].

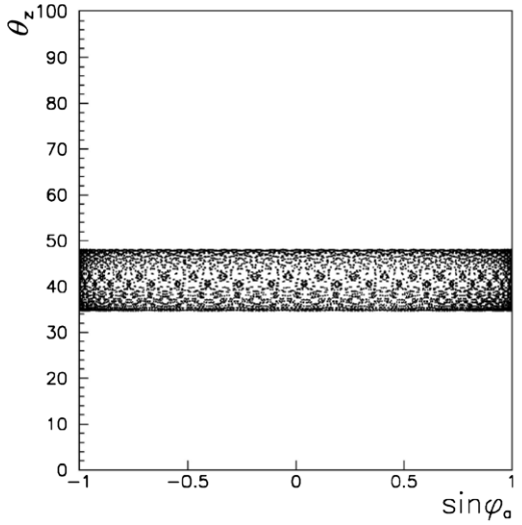

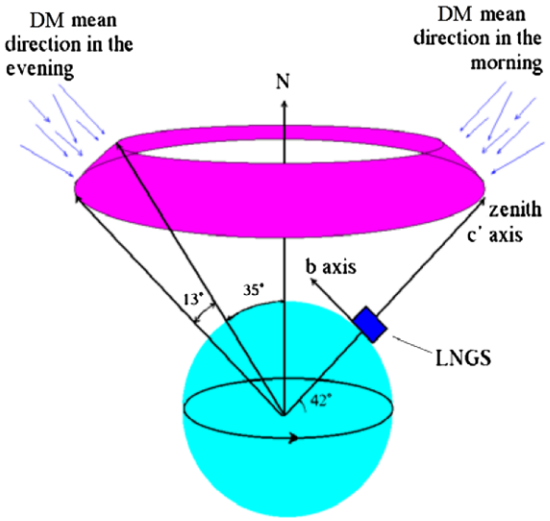

Fig. 1 *Left*: the various directions in the sky of the detector galactic velocity $\vec{v}_d(t)$ calculated for three years as viewed in the coordinate frame located to the North pole (see text). *Right*: schematic representation of the experimental approach mentioned in the text. The detector is considered here as placed at the Gran Sasso National Laboratory (LNGS) with the axis in the vertical direction and another axis pointing to the North. The area in the sky from which the DM particles are preferentially expected is *highlighted* [77]

$\vec{v}_d(t)$ calculated for three years exploiting this useful coordinate frame. As it can be seen, the direction of the $\vec{v}_d(t)$ is confined in the strip: $0 < \varphi_a(t) \leq 2\pi$, $34.5° < \theta_z(t) < 48.1°$. Every point in this strip represents the mean DM arrival direction at a certain t.

Since the "polar-zenith" angle, θ_z, is always near 40°, it is convenient to consider an experiment performed at a latitude similar to, e.g., the latitude of the Gran Sasso National Laboratory (LNGS) of I.N.F.N. (42°27′ N latitude and 13°10′50″ E longitude). In fact, at a certain time of the day the DM particles come mainly from the top, while 12 h later they come near the horizon and from North (see Fig. 1(right)). Thus, if a scintillator with an anisotropic light yield is considered, a suitable arrangement for such an experiment is to install the setup with the detectors' axis having the largest quenching factor value in the vertical direction, and with the axis having the smallest quenching factor value towards the North. In this way, the behavior of the energy spectrum of the DM induced nuclear recoils diurnally varies and, therefore, also the counting rate. A similar approach can be repeated also when considering the anisotropic response of the scintillation decay kinetics. In practice, the investigation can be performed as a function of $\vec{v}_d(t)$ for both the anisotropic features (light output and scintillation decay time) of the detector.

As an example, in the last part of this section we will calculate the effect expected when considering the anisotropic light output of the $ZnWO_4$ detector. In this case, the recoil nuclei induced by the DM candidates considered here could be discriminated from the electromagnetic events thanks to the expected variation of their detected energy[2] distribution during the day [77]. This case has been discussed in Ref. [77] and the expected counting rate of the signal, in the window (E_1, E_2) of the detected energy, has been determined as a function of the time t:

$$
\begin{aligned}
&R(E_1, E_2, t)\\
&= \int d^3\vec{v} \int d\Omega_{\rm cm} \frac{\xi\rho_0 N_n}{m_{\rm DM}} |\vec{v}| f\big[\vec{v} + \vec{v}_d(t)\big] \frac{d\sigma_n}{d\Omega_{\rm cm}}\\
&\quad \times \frac{1}{2}\Bigg[\mathrm{erf}\Bigg(\frac{q_n(\Omega_{\rm out})E_n - E_1}{\sqrt{2}\Delta}\Bigg)\\
&\quad - \mathrm{erf}\Bigg(\frac{q_n(\Omega_{\rm out})E_n - E_2}{\sqrt{2}\Delta}\Bigg)\Bigg]
\end{aligned}
$$

where:

(i) $\frac{\xi\rho_0}{m_{\rm DM}}|\vec{v}| f[\vec{v} + \vec{v}_d(t)]$ is the flux of the considered DM candidate. In particular, ξ is the fraction of the local DM halo density (ρ_0) of the considered candidate; $m_{\rm DM}$ is the mass of the DM candidate. Finally, $f[\vec{v} + \vec{v}_d(t)]$ is the DM velocity distribution in the galactic rest frame; $\vec{v}_d(t)$ is the detector velocity in this reference frame and $\vec{v}$ is the velocity of the DM candidate in the laboratory frame (i.e., $\vec{v}_g = \vec{v} + \vec{v}_d(t)$ is the DM particle velocity in the galactic rest frame);

(ii) N_n is the number of target-nuclei of the nth species per mass unit;

[2]The detected energy is in terms of gamma/beta calibrations, and is generally quoted in keV electron equivalent, hereafter simply keV. It is connected to the recoil nuclear energy by means of a quenching factor (see text).

(iii) $\Omega_{\rm cm} = (\mu, \xi)$ is the nuclear recoil direction in the center of mass (c.m.) frame;
(iv) $\frac{d\sigma_n}{d\Omega_{\rm cm}} = \frac{\sigma_n}{4\pi} F_n^2(q^2)$ is the differential cross section in the c.m. frame, which is assumed to be isotropic. In particular, σ_n is the point-like cross section; $F_n^2(q^2)$ is a form factor, which accounts for the finite sizes of the nucleus, and $q^2 = 2m_n E_n$ is the momentum transfer squared;
(v) $E_n = \frac{1}{2} m_{\rm DM} v^2 \frac{4 m_n m_{\rm DM}}{(m_n + m_{\rm DM})^2} \frac{1-\mu}{2}$ is the kinetic energy of the recoiling nucleus (with mass m_n) in the laboratory frame;
(vi) $q_n(\Omega_{\rm out})$ is the quenching factor which depends on the output direction of the nuclear recoil in the laboratory frame; $(\Omega_{\rm out}) = (\gamma, \phi)$ is the corresponding solid angle. In particular, $q_n(\Omega_{\rm out}) = q_{n,x} \sin^2\gamma \cos^2\phi + q_{n,y} \sin^2\gamma \sin^2\phi + q_{n,z} \cos^2\gamma$; there $q_{n,i}$ indicates the quenching factor value for a given nucleus (n) with respect to the ith axis of the anisotropic crystal;
(vii) Δ is the detector energy resolution.

Both E_n and $\Omega_{\rm out}$ are functions of $\vec{v}$ and $\Omega_{\rm cm}$. The generalization to the case of a detector with multi-atomic species is straightforward.

Many quantities in the above formula are model dependent and a model framework has to be fixed among the many possible; this is identified not only by general astrophysical, nuclear and particle physics assumptions, but also by the adopted set of parameter values.

In the following example, for simplicity, we fix a set of assumptions and of values, without considering the effect of the existing uncertainties on each one of them; obviously, the reader should keep in mind the uncertainties associated to the presented results. Thus, only the particular case of DM with dominant spin-independent (SI) coupling is considered. The DM-nucleus elastic cross section, σ_n, is written in terms of the DM elastic cross section on a nucleon, σ_p, assuming a scaling law:

$$\sigma_n = \sigma_p \left(\frac{M_n^{\rm red}}{M_p^{\rm red}} \cdot A \right)^2 = \sigma_p \left(\frac{m_p + m_{\rm DM}}{m_n + m_{\rm DM}} \cdot \frac{m_n}{m_p} \cdot A \right)^2 .$$

Here $M_n^{\rm red}$ ($M_p^{\rm red}$) is the reduced mass of the nucleus(nucleon)-DM system. Moreover, again for simplicity we assume:

(i) a simple exponential form factor: $F_n^2(E_n) = e^{-E_n/E_0}$, where $E_0 = \frac{3(\hbar c)^2}{2 m_n r_o^2}$ and $r_0 = 0.3 + 0.91 \sqrt[3]{m_n}$ (r_0 is the radius of the nucleus in fm when m_n is given in GeV);
(ii) a simple spherical isothermal DM halo model with $f(\vec{v}_g) = \frac{1}{\pi^{3/2} v_0^3} e^{-(|\vec{v}_g|/v_0)^2} \Theta(v_{\rm esc} - |\vec{v}_g|)$, where v_0 is the DM local velocity (here assumed equal to 220 km/s), $v_{\rm esc}$ is the escape velocity of the Galaxy (here assumed equal to 650 km/s) and Θ is the Heaviside function;
(iii) a value of 0.3 GeV/cm^3 for the local DM halo density ρ_0;
(iv) values of the Zn, W and O quenching factors with respect to the three axes of the $ZnWO_4$ crystal obtained by the method described in Ref. [90] considering the data of the anisotropy to α particles (see later).

As an example, on the basis of the model framework given above, we have calculated the effect achievable when exploiting the DM directionality approach with a $ZnWO_4$ detector for the cases of DM particles with $\xi\sigma_p = 5 \times 10^{-5}$ pb. The result is shown in Fig. 2 for the cases $m_{\rm DM} =$ 10 GeV (up) and 50 GeV (down), where the dependence of the expected rates in the 2–3 keV (left) and 6–7 keV (right) energy windows on the DM arrival direction with respect to the crystal axes is given; there is a clear dependence on φ_a, and therefore on the sidereal time, that gives a diurnal variation of the rate because of the Earth's daily rotation.

As previously mentioned, also the pulse shape of the scintillation events induced by heavy particles depends on the energy and on the direction of the impinging particles with respect to the crystal axes. Such a dependence can be quantified by using approaches that give a parameterization of the pulse shape, as e.g. the optimal filter method [91], but many other approaches are also possible. This peculiarity of $ZnWO_4$ scintillation detectors can provide a further tool to study the directionality signature with a completely different approach with respect to the case of light output anisotropy; it will be discussed in Sect. 4.3.

3 The $ZnWO_4$ anisotropic scintillator

As mentioned, the inorganic $ZnWO_4$ scintillator can fit the main requirements to reach competitive experimental sensitivities: suitable anisotropic features, high radiopurity, low energy threshold, large mass, suitable sensitivity to different masses of the considered DM candidates and high stability of the running conditions. In the comparison with the anthracene detector, originally suggested in Ref. [76], the $ZnWO_4$ offers a higher atomic weight and the possibility to realize crystals with masses of some kg. Moreover, three target nuclei with very different masses are present in this detector (Zn, W and O), giving sensitivity to both small and large mass for the considered DM candidates.

The luminescence of $ZnWO_4$ was studied sixty years ago [92]. Large volume $ZnWO_4$ single crystals of reasonable quality were grown [93] and studied as scintillators in the eighties [94, 95]. Further development of large volume high quality radiopure $ZnWO_4$ crystal scintillators is described in [96–98]. The main properties of the $ZnWO_4$ scintillators are given in Table 1.

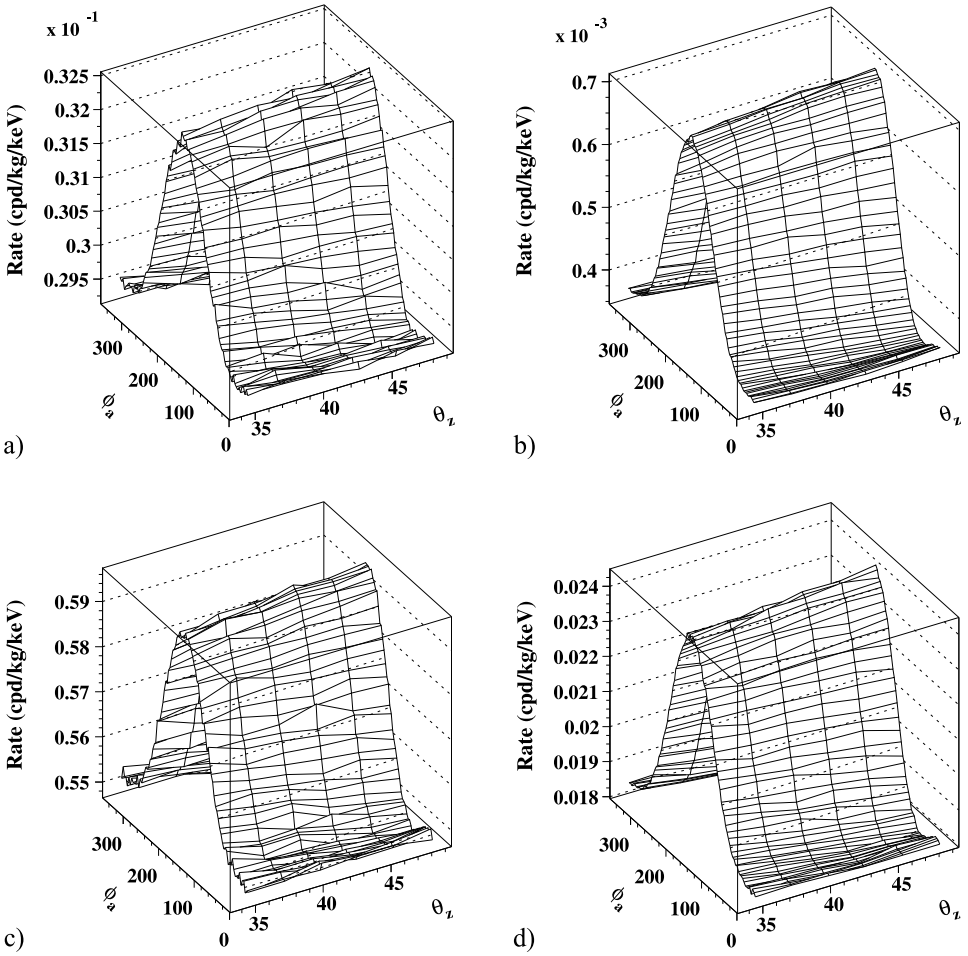

Fig. 2 Some examples of the expected rate for the case of a DM particle inducing just nuclear recoils and $\xi\sigma_p = 5 \times 10^{-5}$ pb in the model framework assumed in the text. In particular, these examples refer to the case of a DM particle with mass equal to 10 GeV (*up*) or 50 GeV (*down*). The dependences of the expected rates in the 2–3 keV (*left*) and 6–7 keV (*right*) energy windows are shown as a function of the detector's (or Earth's) possible velocity directions. There is a strong dependence on the "polar-azimuth" φ_a that induces a diurnal variation of the rate

Table 1 Properties of the $ZnWO_4$ crystal scintillators

Density (g/cm^3)	7.87
Melting point (°C)	1200
Structural type	Wolframite
Cleavage plane	Marked (010)
Hardness (Mohs)	4–4.5
Wavelength of emission maximum (nm)	480
Refractive index	2.1–2.2
Effective average decay time (μs)	24

The material is non-hygroscopic and chemically resistant. The first low background measurement with a small $ZnWO_4$ sample (mass of 4.5 g) was performed in the Solotvina underground laboratory (Ukraine) at a depth of ≈1000 m of water equivalent (m.w.e.) in order to study its radioactive contamination, and to search for double beta decay of zinc and tungsten isotopes [99]. In this work a possibility to use the dependence of $ZnWO_4$ scintillation pulse shape on direction of irradiation by high ionizing particles to search for diurnal modulation of DM particles inducing recoils was pointed out for the first time. More recently, radiopurity and double beta decay processes of zinc and tungsten have been further studied also at LNGS using $ZnWO_4$ detectors with masses 0.1–0.7 kg [80, 81, 100, 101].

3.1 Anisotropic features and pulse shape analysis (PSA) in $ZnWO_4$

As previously mentioned, the study of the directionality with the $ZnWO_4$ detectors is based on the anisotropic properties of these scintillators. In particular, the reachable sensitivity of the directionality approach will depend on the anisotropic features of the detectors in response to the low energy nuclear recoils induced by the DM candidate particles considered here. Measurements with low energy nuclear recoils have not been performed yet, but measurements with α particles have shown that the light response and the pulse shape of a $ZnWO_4$ scintillator depend on the impinging direction of α particles with respect to the crystal axes. Figure 3 shows the dependence in a $ZnWO_4$ crystal of the α/β light ratio (quenching factor) on energy and direction of the α beam relatively to the crystal planes [99]. The $ZnWO_4$ crystal was irradiated in the directions perpendicular to the (010), (001)

and (100) crystal planes (directions 1, 2 and 3, respectively in Fig. 3).

As shown in Fig. 3, the quenching factor for α particles measured along direction 1 is about 1.5 times larger than that measured along direction 2, and about 1.4 times larger than that measured along direction 3. Measurements of the quenching factor and of the anisotropic effect down to tens of keV have also been reported for other anisotropic crystals e.g. in [78, 79], showing an effect still quite appreciable. Moreover, it has also been verified that such an anisotropy is not present in case of electron excitation.

On the basis of the anisotropic behaviour of the $ZnWO_4$ to α radiations, similar effect can also be expected in the case of nuclear recoils; this can be quantified through the calibrations of the $ZnWO_4$ detectors with neutron sources, changing the orientation of the crystal with respect to the direction of the impinging neutrons. It is expected that quenching factor will be different depending both on the direction of the recoiling nucleus with respect to crystal axes and on the nucleus itself (Zn, W or O). Dedicated measurements are in preparation. Since no estimates for such quenching factors in the keV region respect to the crystal's axes are available (actually, measurements of the average quenching factors in $ZnWO_4$ for recoiling nuclei are reported in [102]), in this paper their values have been calculated by applying the method described in Ref. [90] considering the data of the anisotropy to α particles. The results are given in Table 2 for

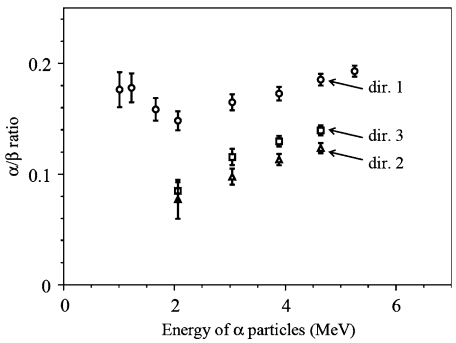

Fig. 3 Dependence of the α/β ratio on energy of α particles measured with $ZnWO_4$ scintillator. The crystal was irradiated in the directions perpendicular to (010), (001) and (100) crystal planes (directions 1, 2 and 3, respectively). The anisotropic behaviour of the crystal is evident [99]

Table 2 Quenching factors for O, Zn and W ions with energy 5 keV for different directions in $ZnWO_4$ crystal. Systematic uncertainties are estimated on the level of 20 % using data of [90]

Ion	Quenching factor		
	dir. 1	dir. 2	dir. 3
O	0.235	0.159	0.176
Zn	0.084	0.054	0.060
W	0.058	0.037	0.041

recoils with energy of 5 keV. One should also note that in the work [102] quenching factors for recoiling O, Zn and W nuclei were measured, but they cannot be directly compared with the data of Table 2 because they represent some average values for different ions and different directions.

As stated above, the anisotropy of the light response of the $ZnWO_4$ scintillator disappears in case of electron excitation. Moreover, as demonstrated in Ref. [99], the dependence of the pulse shapes on the type of irradiation in the $ZnWO_4$ scintillator allows one to discriminate $\gamma(\beta)$ events from those induced by α particles. As an example, the PSA can be applied in order to identify and evaluate the α background during the detector development. In particular, by applying the optimal filter method [91], in Ref. [99] the so-called shape indicator, *SI*, was calculated for each pulse to obtain the numerical characteristic of scintillation pulse: $SI = \sum_k f(t_k)P(t_k)/\sum_k f(t_k)$, where the sum is over time channels k, $f(t_k)$ is the digitized amplitude (at the time t_k) of a given signal and $P(t_k)$ is the weight function. This latter was defined as: $P(t) = \{r_\alpha(t) - r_\gamma(t)\}/\{r_\alpha(t) + r_\gamma(t)\}$, where $r_\alpha(t)$ and $r_\gamma(t)$ are the reference pulse shapes for α particles and γ quanta. The result is shown in Fig. 4 [80]. As also e.g. in NaI(Tl), the $ZnWO_4$ shows a practically 100 % discrimination between high energy α particles and the γ rays (β particles).

As a measurement of the discrimination capability, the following parameter can be used: $m_{PSA} = |SI_\alpha - SI_\gamma|/(\sigma_\alpha^2 + \sigma_\gamma^2)^{1/2}$, where SI_α and SI_γ are mean *SI* values of α particles and γ quanta distributions (which are well described by Gaussian functions), σ_α and σ_γ are the corresponding standard deviations. Typical values of the parameter m_{PSA} are 4–5 [99] in the few-MeV electron equivalent region. Obviously, the discrimination power for few keV nuclear recoils

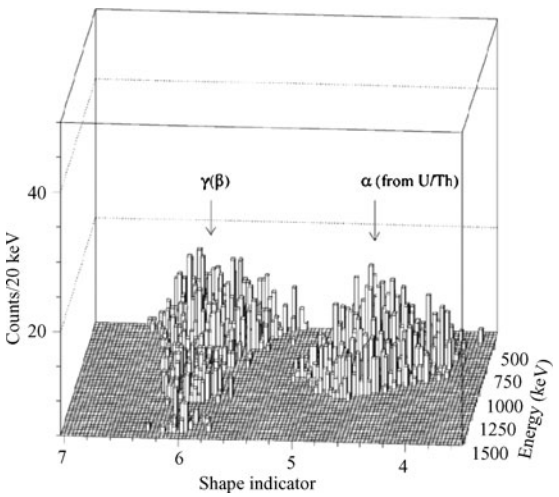

Fig. 4 Three-dimensional distribution of background events accumulated with a $ZnWO_4$ crystal versus the energy and the shape indicator (see text). The population of the α events belonging to the internal contamination by U/Th is clearly separated from the $\gamma(\beta)$ background. The energy scale refers to the calibrations with γ sources [80]

is expected to become significantly lower than 100 %, as it happens in case of other scintillators. However, this feature can be well quantified in the case of $ZnWO_4$ scintillator by means of calibrations with neutron sources both at normal and low operating temperature, and applied to the data analysis.

By the PSA analysis it is also possible to point out the anisotropic behaviour of the pulse shape in case of heavy particles impinging on a $ZnWO_4$ detector. As an example, we show in Fig. 5 the dependence of the *SI* on the energy and on the impinging direction of the α particles obtained with a $ZnWO_4$ scintillator irradiated in the directions 1, 2 and 3 [99]. Also in this case, the anisotropic behaviour of the crystal's response is evident.

Thus, a sizeable anisotropic behaviour of the pulse shape can also be expected for low energy nuclear recoils, providing a further tool to study the directionality approach. The realistic use of this pulse shape feature at low energy requires a high discrimination power and relies on an optimized and increased light production and collection (i.e. improved performances of the $ZnWO_4$ crystals, of the light collection and of suitable photo devices). Thus, the general present and future R&Ds will also allow a precise evaluation about the exploitation of such an additional tool.

3.2 Light yield and energy threshold

For kinematic reasons, as result of elastic scattering with a DM particle with mass of few GeV or larger, the target nucleus (Zn, W or O) will recoil with energy of few keV (electron equivalent scale). A competitive experiment for the DM investigation needs a low energy threshold and also an efficient reduction of the residual noise near the software energy threshold in order to point out the scintillation signal produced by the interaction with DM particles. The reachable energy threshold depends both on the scintillator light output (number of photoelectron/keV), and on the level of the noise near the software energy threshold. In fact, the contribution of the noise (mostly single photoelectron pulses) sharply decreases when increasing the number of available photoelectrons while the efficiency of the noise rejection (see Sect. 4.3) increases.

In a recent experiment, not optimized for the low energy region, a $ZnWO_4$ crystal has been used to study the double electron capture of ^{64}Zn with an energy threshold of 10 keV [81]. An improved light collection and a reduction of the photomultiplier (PMT) noise can be obtained when the $ZnWO_4$ scintillator is directly coupled—on opposite sides—to two low-background PMTs with high quantum efficiency, working in coincidence at single photoelectron level. These peculiarities are satisfied by the new low-background Hamamatsu PMTs with high quantum efficiency and low dark current recently developed for the DAMA/LIBRA experiment (see Ref. [104] and Sect. 4.2).

Moreover, in Ref. [99] a substantial improvement of light collection (∼40 %) and energy resolution was achieved by placing the crystal in silicone oil (refraction index ≈1.5). In Ref. [105] the light yield of $ZnWO_4$ was measured with the help of silicon photodiodes as 9300 photons/MeV (which is ∼23 % of NaI(Tl) light yield).

A large improvement in the light yield can also be obtained by decreasing the operational temperature of the $ZnWO_4$ scintillator. The relative scintillation intensity and decay kinetics of $ZnWO_4$ were studied [106] below 300 K. The variation of the light output of $ZnWO_4$ in the temperature interval 100–300 K has been measured in Ref. [106] and is shown in Fig. 6. The temperature dependence of the decay time constants of $ZnWO_4$ has been measured using a γ source as well [106]. The decay time constants remain quite unchanged down to tens of K.

Thus, space for further improvements on the response and on the software energy threshold is possible.

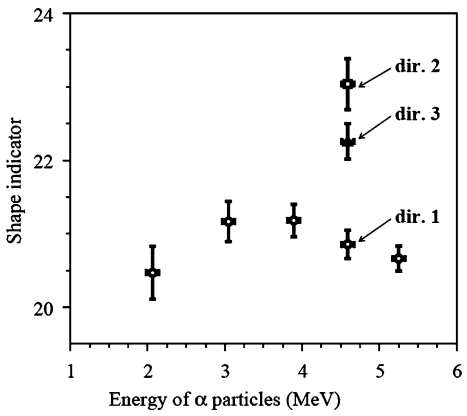

Fig. 5 Dependence of the shape indicator (see text) on the energy and on the directions of α particles relatively to the main (010), (001) and (100) crystal planes of $ZnWO_4$ (directions 1, 2 and 3, respectively) [99]. Similar behavior has been observed also with $CdWO_4$ scintillators [103]

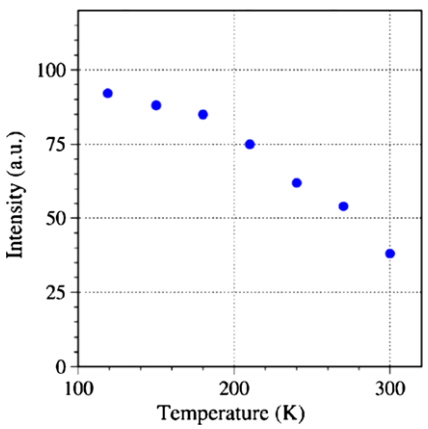

Fig. 6 Temperature dependence of the light output of the $ZnWO_4$ crystal scintillator for excitation with ^{241}Am α particles [106]

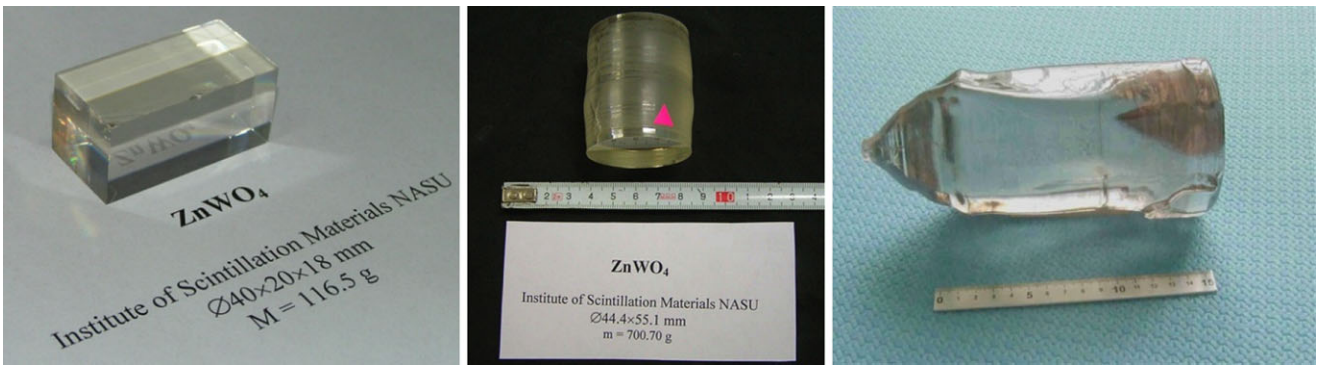

Fig. 7 Three of the $ZnWO_4$ crystal scintillators recently developed [80]. Two $ZnWO_4$ samples (*left* and *middle pictures*) have been grown in the Institute of Scintillation Materials (Kharkiv, Ukraine). The crystal in the *right picture* has been produced in the Nikolaev Institute of Inorganic Chemistry (Novosibirsk, Russia); it is ≈8 cm in diameter and ≈15 cm length of cylindrical part

3.3 Radiopurity of $ZnWO_4$ scintillators

R&D developments have been recently performed with the aim to develop highly radiopure $ZnWO_4$ crystals [80]. The growth of the crystals, the scintillation properties, the pulse shape discrimination capability, their anisotropic properties, their residual radioactive contamination, their possible applications have been studied [80, 96–98, 100, 101]. Different $ZnWO_4$ prototypes have been investigated (three of them are shown in Fig. 7): the results are excellent and the R&D is still ongoing.

The measured radioactive contamination is [80]: less than 0.002 mBq/kg for ^{228}Th and ^{226}Ra (∼0.5 ppt for ^{232}Th and ∼0.2 ppt for ^{238}U, assuming the secular equilibrium of the ^{232}Th and ^{238}U chains), less than 0.02 mBq/kg for ^{40}K; in particular, a total α activity of 0.18 mBq/kg has been measured. The radioactive contamination of the samples of $ZnWO_4$ crystals approaches that of specially developed low background NaI(Tl); moreover, $ZnWO_4$ crystals having higher radiopurity could be expected in future realizations. In particular, new careful selections and purifications of the initial materials have to be carried out since the radioactive contaminations of the initial compounds, used in the crystal growth, give considerable contribution to the radioactivity of the crystal scintillators. One could expect that vacuum distillation and filtering could be very promising approaches [107–109] to obtain high purity zinc, while zone melting could be used for additional purification of tungsten. Obviously all the more accurate techniques for the screening, purification and protection from environment of all the materials in every stage should be applied. In addition, preliminary investigations of cadmium tungstate ($CdWO_4$) crystal scintillators showed that the segregation of radioactive elements (U, Th, Ra, K) is very low during $CdWO_4$ crystal growth [110]; one could expect analogous properties also in $ZnWO_4$ (very similar compound to $CdWO_4$).

After the final production of the crystal, an additional tool for the investigation and reduction of the residual background can be provided by using a multi-detector set-up. In fact, the effect searched for should be present only in the *single-hit* events (that is, each detector has all the others in the same installation as veto) and not in the *multiple-hit* events. Thus, the event pattern will contribute both to the signal identification and to the study of the background.

4 The ADAMO (anisotropic detectors for dark matter observation) project

In the following we will describe the potentiality of an experiment based on an array of ultra-low-background $ZnWO_4$ scintillators housed in a suitable low background experimental set-up located deep underground.

4.1 Single module structure

The structure of the single detector module can be chosen taking into account the specific requirements for the energy threshold and for background reduction. Recently, in the experiment [100] for the study of 2β decays of Zn and W isotopes with $ZnWO_4$ detectors, the configuration shown in Fig. 8 has been used. In particular, the $ZnWO_4$ crystal was fixed inside a cavity of ∅49 × 59 mm in the central part of a polystyrene light-guide 66 mm in diameter and 312 mm in length. The cavity was filled up with high purity silicone oil with the function of increasing the light collection. The light-guide was optically connected, on the opposite sides, to two low radioactive PMTs. The light-guide was wrapped by PTFE reflection tape. The long light-guide allowed the reduction of the PMTs contribution to background, but at the same time made worse the light collection. Nevertheless, as stated above, the energy threshold reached with this configuration was already 10 keV.

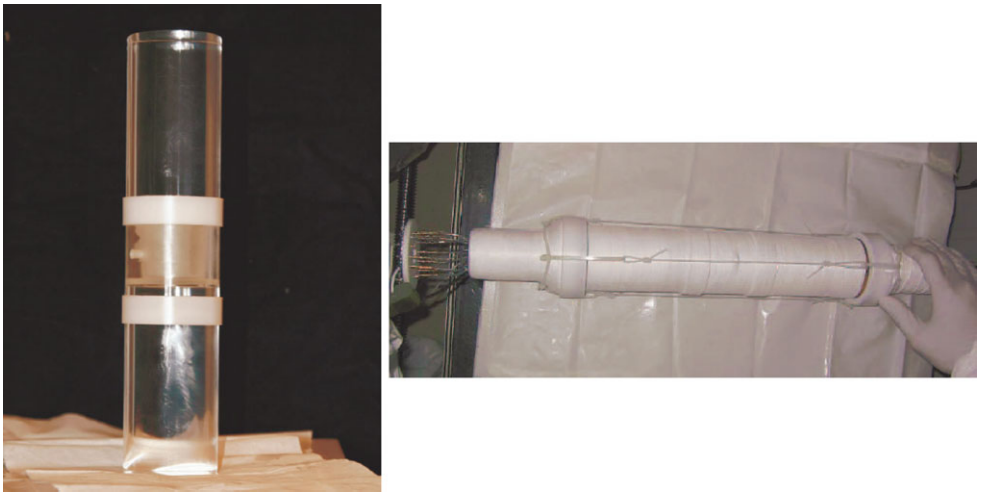

Fig. 8 The experimental configuration used in Ref. [100] before the light guide was wrapped by PTFE reflection tape (*left*) and after wrapping (*right*). This is one of the possible configurations for the single module structure of the ADAMO experiment

Since the eighties it has been demonstrated that it is possible to grow large volume $ZnWO_4$ single crystals of comparatively high quality [93]. With the present technology $ZnWO_4$ crystals with a mass of about 8 kg and typical sizes of $\varnothing 8 \times 20$ cm can be produced for the proposed experiment [98]. They can be viewed by two low background PMTs working in coincidence; this will imply the increase of the light collection and the reduction of the PMT noise near energy threshold. The PMTs recently developed by Hamamatsu for the 2010 upgrade of DAMA/LIBRA set-up can be used. They have: $\langle$Quantum Efficiency$\rangle \approx 39$ %, dark current less than 100 Hz in the best PMTs and, as regard the radiopurity, (0.43 ± 0.06) Bq/kg for ^{226}Ra, (47 ± 10) mBq/kg for ^{235}U, (83 ± 17) mBq/kg for ^{228}Th and (0.54 ± 0.16) Bq/kg for ^{40}K (mean values and standard deviations calculated on several PMTs).

Several experimental configurations can be preliminarily tested to understand if the light-guide can be reduced or even eliminated. Another possibility that can be tested is the replacement of the silicone oil with high purity liquid scintillator. In principle, the latter can show similar capabilities of increasing the light collection as the silicone oil, and can be used as anticoincidence detector. In fact, the fast (few ns) scintillation pulses produced by the liquid scintillator can be easily distinguished from the long ($\tau \approx 24$ μs) pulses of the $ZnWO_4$ scintillator. This technique was already successfully applied in the low background experiment to search for double beta decay of ^{116}Cd with the help of enriched in ^{116}Cd cadmium tungstate crystal scintillators [111].

4.2 Schematic design of the full set-up

Profiting of the experience of the DAMA collaboration with the DAMA/LIBRA set-up [112] and of the proved success of this detector configuration and of the shielding for the background reduction, a similar scheme can be adopted also for the proposed experiment.

As seen in the previous section, $ZnWO_4$ detectors with $\varnothing 8 \times 20$ cm size can be produced. If two PMTs are coupled to the detectors using two 10 cm long Tetrasil-B light-guides, the total size of the single module will be about $\varnothing 8 \times 80$ cm (also considering the PMTs and voltage dividers). Hence, 25 of such modules placed in a 5-rows by 5-columns matrix can be installed in a sealed low radioactive copper box with $45 \times 45 \times 90$ cm^3 size. Obviously, the final size of the copper box could be slightly different depending on the final configuration of the single detector module (i.e. either using or not using the light-guides, the silicone oil, etc.). The low radioactive copper box, sealed and continuously flushed with high purity (HP) N_2 gas, can be placed in the centre of a multi-ton, multi-component low radioactive passive shield (similar to the one described in Ref. [112]) deep underground. In particular, outside the Cu box, the passive shield can be composed by 10 cm of low radioactive copper, 15 cm of low radioactive lead, 1.5 mm of cadmium and more than 20 cm of polyethylene/paraffin. A sealed Plexiglas box, continuously flushed with HP Nitrogen gas can enclose the passive shield. Moreover, about 1 m concrete (made from the Gran Sasso rock material) can almost fully surround this passive shield, acting as a further neutron moderator. On the top of the multi-tons, multi-component shield a glove-box, continuously maintained in HP Nitrogen atmosphere, will be directly connected through Cu pipes to the inner Cu box; these pipes allow the insertion of radioactive sources holders for calibrating the detectors in the same running condition and down to the keV region.

The fragmentation of the set-up is useful for background identification and rejection; in fact, for example, the signal should be present only in the events where just one detector of many fires since the multi-interaction probability of DM particles is negligible.

The electronic chain and the DAQ system can be similar to those already in operation in the DAMA/LIBRA set-up [112], that allow the recording both of the *single-hit*

events (those events where just one detector of many actually fires) and of the *multiple-hit* events (those events where more than one detector fire). The trigger of each detector can be issued by the coincidence of the pulses of the two PMTs working at single photoelectron threshold and the pulse profiles of the two PMTs can be recorded by Waveform Analyzers. Moreover, as the DAMA/LIBRA and the DAMA/NaI experiments, the proposed set-up will take data up to the MeV scale, despite the optimization will be made for the lowest energy region. The linearity and the energy resolution of the detectors at low and high energy will be investigated by using several sources down to the software energy threshold.

A hardware/software system to monitor the running conditions will be operative and self-controlled computer processes will automatically control several parameters and will manage alarms. The DAQ will also record—together with the production data—the information coming from the monitoring system.

4.3 Data analysis

As previously stated, as result of elastic scattering with the DM candidate particles considered here the target nucleus will recoil with energy of few keV (electron equivalent scale). Moreover, because of the weak interaction of DM particles, the probability of a multiple interaction in a multi-detector setup (*multiple-hit* events) is negligible. For these arguments, the expected effect from the directionality approach has to be searched for in the class of the *single-hit* events with energy in the few keV region. Hence, the *multiple-hit* events do not contribute to the directionality signal resulting in an effective reduction of the background.

Procedures similar to those in Ref. [112] can be also applied to remove possible tails of noise events near software energy threshold. In fact, these latter pulses populate the region near the energy threshold, but their number sharply decreases when increasing the number of available photoelectrons. In particular, in the proposed experiment the detectors will be seen by two PMTs working in coincidence and this already strongly reduces the noise contribution. In particular, the residual noise will be removed profiting of the very different time distribution of the noise events (fast pulses with decay time of order of tens of ns) and the $ZnWO_4$ scintillation pulses (typical decay time of about 24 μs).

The *single-hit* events can be analysed to study the DM signal directionality by exploiting the anisotropic light yield of the $ZnWO_4$ detectors and the consequent expected time-variation of the low energy spectrum. In fact, as discussed above, the expected counting rate in a given energy window depends on the impinging direction of the DM particles with respect to crystal axes, and therefore (for a detector at rest on the Earth) on the sidereal time. An example of the reachable sensitivity with this method will be given in the following section.

Another approach is possible. In fact, as previously discussed, in addition to the light yield also the pulse shape of the events induced by heavy particles shows an anisotropic effect. Considering this feature as appreciable also for keV nuclear recoil, the following—in principle powerful—approach can be pursued as well. In fact, since the direction of the impinging DM particles with respect to the crystal axes varies during the day because of the Earth rotation, one expects that in the low energy region, where the recoil signals induced by the DM candidates considered here are expected, the events pulse shape will depend on time. Obviously, this dependence will have a period equal to a sidereal day. After collecting a suitable exposure, the data analysis can be performed considering all the data as collected in a single sidereal day (that is, a single period). This latter can be divided in a suitable number of time bin, n, and for each time bin one can calculate the average value of the variable, $V(n)$, chosen for the parameterization of the pulse shape (e.g. the *SI*), and the associated standard deviation. In case of absence of DM signal, we expect that the calculated $V(n)$ will be in agreement each others because: (i) as regards heavy particles or whatever possible background (e.g. neutron) that can induce nuclear recoils, their impinging direction is not expected to vary during the sidereal day; (ii) as regard the electromagnetic background, the previous argument still holds and in addition no dependence of the pulse shape on the direction of the impinging gamma/beta particles has been measured. On the other hand, in case of the DM candidates considered here, the signal can be pointed out by possible incompatibilities among the $V(n)$ variables calculated for the different time bins of the sidereal day, in the low energy region. Moreover, the measured $V(n)$ have also to satisfy a time behaviour—that is, $V(n)$ vs. n—with a well defined structure. It is worth noting that compatibility among the calculated $V(n)$ is instead expected when considering events in higher energy regions (or *multiple-hit* events), where the considered DM candidate particles cannot give an appreciable signal. This latter point can be a good test of the proposed analysis.

5 Example of the reachable sensitivity in a given scenario

As mentioned, the directionality approach can offer a way, largely independent on other additional assumptions, for pointing out the presence of the considered DM candidate particles; however, in the following a specific simplified model framework is considered to derive some kinds of quantitative evaluations.

The sensitivity reachable—for the model scenario described in Sect. 2—by the ADAMO project (200 kg of

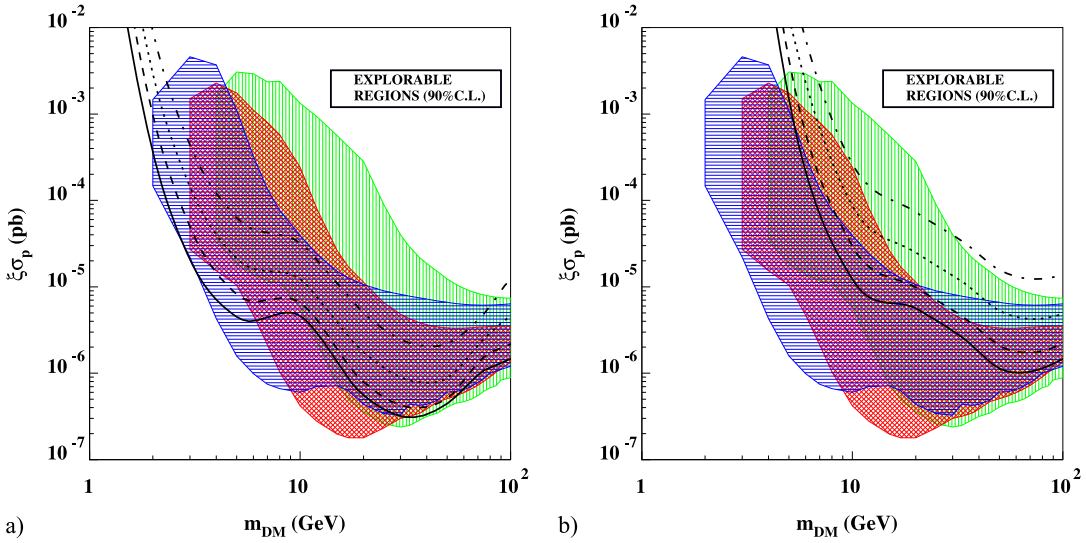

Fig. 9 Sensitivity curves (*black online*) at 90 % C.L. reachable by the ADAMO project for DM candidates inducing just nuclear recoils in the model scenario given in the text by exploring the directionality approach. Four possible background levels in the low energy region are considered as given in the text as well as two possible software energy thresholds: 2 keVee in (**a**) and 6 keVee in (**b**). There $m_{\rm DM}$ is the particle mass, σ_p is the spin-independent cross section on nucleon and ξ is the fraction of the DM local density of the considered candidate. In the figures there are also shown allowed regions obtained in Ref. [113] by performing a corollary analysis of the 9σ C.L. DAMA model independent result in terms of scenarios for DM candidates inducing just nuclear recoils. In particular, the three (colored) hatched regions denote the DAMA annual-modulation regions in 3 different instances: (i) without including the channeling effect [(*green*) *vertically-hatched region*], (ii) by including the channeling effect according to Ref. [114] [(*blue*) *horizontally-hatched region*)], and (iii) without the channeling effect but using the energy-dependent Na and I quenching factors as established by the procedure given in Ref. [90] [(*red*) *cross-hatched region*]. See text

$ZnWO_4$, 5 years of data taking and an energy resolution $FWHM = 2.4\sqrt{E[\text{keV}]}$), exploring the directionality approach, is reported in Fig. 9. In particular, two software energy thresholds have been considered: 2 keVee for Fig. 9(a) and 6 keVee for Fig. 9(b). The reachable sensitivity has been calculated considering four possible time independent background levels in the low energy region: 10^{-4} cpd/kg/keV (solid black lines), 10^{-3} cpd/kg/keV (dashed lines), 10^{-2} cpd/kg/keV (dotted lines) and 0.1 cpd/kg/keV (dotted-dashed lines).[3] For the Zn, W and O quenching factors with respect of the three axes of the $ZnWO_4$ crystal we have considered here the values obtained by the method described in Ref. [90] considering the data of the anisotropy to α particles (see Fig. 3). As shown in Fig. 9 the directionality approach can reach—for the DM candidates investigated here and under the given model scenario—a sensitivity to SI cross sections at level of 10^{-5}–10^{-7} pb, depending on the candidate mass between few GeV and hundreds GeV. However, it is worth noting that these plots are model dependent and, thus, always affected by several uncertainties; here, for simplicity, the same scenario described in Sect. 2 has been considered (isothermal halo model, Maxwellian velocity distribution, spin independent interaction, and related assumptions; see Sect. 2 for details). In Fig. 9 the allowed regions (7.5σ from the null hypothesis) obtained by performing a corollary analysis of the DAMA model independent result in term of the scenarios described in Ref. [113] are also reported; in particular, three instances were considered for the Na and I quenching factors.

As shown, under the given assumptions, the proposed project on directionality can reach for DM candidates inducing just recoils sensitivities not far from those of the DAMA/LIBRA positive model independent result [2, 3], and of the CoGeNT [15] and CRESST [16] positive hints. Obviously, when entering in model dependent comparison, significant uncertainties exist.

6 Conclusions

The possibility of a pioneering experiment with anisotropic $ZnWO_4$ detectors to further explore, with the directional-

[3] A background counting rate of the order of 3.5 cpd/kg/keV was obtained at low energies in the mentioned previous experiment with a $ZnWO_4$ detector [80]. It was evaluated that most of the low energy counting rate can be ascribed to external background [80]. Therefore, a large margin of improvement is possible; in particular, a value of 0.1 cpd/kg/keV is estimated by Monte Carlo simulation assuming the already achieved intrinsic radioactive contamination of $ZnWO_4$ crystal scintillators (see data for the crystal ZWO-2 presented in Table 3 of Ref. [80]).

ity approach, DM candidate particles that scatter off target nuclei has been addressed. The features and the potentiality of these detectors can permit to reach—in some of the many possible scenarios and for the DM candidates considered here—sensitivities not far from that of the DAMA/LIBRA positive result [2, 3] and of the CoGeNT [15] and CRESST [16] recent possible positive hints. In case of success such an experiment can obtain an evidence for the presence of such DM candidate particles in the galactic halo with a new approach and will provide complementary information on the nature and interaction type of the DM candidate(s). In case of negative results the experiment would favour other kinds of astrophysical, nuclear and particle physics scenarios for the DM candidates considered here and/or other DM candidate particles, interaction types and scenarios which can account as well for the 9σ C.L. DM model independent evidence already observed by the DAMA experiments.

In all cases this experiment would represent a first realistic attempt to investigate the directionality approach through the use of anisotropic scintillators and it could also represent a further activity in the application of highly radio-pure $ZnWO_4$ detector in the field of rare processes.

Acknowledgements The work of F.A. Danevich, D.V. Poda and V.I. Tretyak was supported in part by the Space Research Program of the National Academy of Sciences of Ukraine. Authors are grateful to Ya.V. Vasiliev, V.N. Shlegel and E.N. Galashov from the Nikolaev Institute of Inorganic Chemistry (Novosibirsk, Russia) for kindly provided picture of large $ZnWO_4$ crystal scintillator.

References

1. R. Bernabei et al., Riv. Nuovo Cimento **26**(1), 1 (2003)
2. R. Bernabei et al., Eur. Phys. J. C **56**, 333 (2008)
3. R. Bernabei et al., Eur. Phys. J. C **67**, 39 (2010)
4. K.A. Drukier et al., Phys. Rev. D **33**, 3495 (1986)
5. K. Freese et al., Phys. Rev. D **37**, 3388 (1988)
6. R. Bernabei et al., Eur. Phys. J. C **18**, 283 (2000)
7. R. Bernabei et al., Int. J. Mod. Phys. D **13**, 2127 (2004)
8. K. Freese, M. Lisanti, C. Savage, arXiv:1209.3339v2 [astro-ph.CO]
9. R. Cerulli, Direct detection of dark matter particles, in *Proceedings of Dark Force*, LNF, Frascati, 2012. http://www.lnf.infn.it/conference/dark/
10. R. Bernabei, P. Belli, A. Incicchitti, D. Prosperi, arXiv:0806.0011v2
11. J.I. Collar. arXiv:1204.3559
12. J.I. Collar. arXiv:1106.0653
13. J.I. Collar, arXiv:1103.3481
14. J.I. Collar, arXiv:1010.5187
15. C.E. Aalseth et al., Phys. Rev. Lett. **107**, 141301 (2011)
16. G. Angloher et al., Eur. Phys. J. C **72**, 1971 (2012)
17. R. Bernabei et al., Phys. Lett. B **389**, 757 (1996)
18. R. Bernabei et al., Phys. Lett. B **424**, 195 (1998)
19. R. Bernabei et al., Phys. Lett. B **450**, 448 (1999)
20. P. Belli et al., Phys. Rev. D **61**, 023512 (2000)
21. R. Bernabei et al., Phys. Lett. B **480**, 23 (2000)
22. R. Bernabei et al., Phys. Lett. B **509**, 197 (2001)
23. R. Bernabei et al., Eur. Phys. J. C **23**, 61 (2002)
24. P. Belli et al., Phys. Rev. D **66**, 043503 (2002)
25. R. Bernabei et al., Int. J. Mod. Phys. A **21**, 1445 (2006)
26. R. Bernabei et al., Eur. Phys. J. C **47**, 263 (2006)
27. R. Bernabei et al., Int. J. Mod. Phys. A **22**, 3155 (2007)
28. R. Bernabei et al., Eur. Phys. J. C **53**, 205 (2008)
29. R. Bernabei et al., Phys. Rev. D **77**, 023506 (2008)
30. R. Bernabei et al., Mod. Phys. Lett. A **23**, 2125 (2008)
31. A. Bottino et al., Phys. Rev. D **81**, 107302 (2010)
32. N. Fornengo et al., Phys. Rev. D **83**, 15001 (2011)
33. A.L. Fitzpatrick et al., Phys. Rev. D **81**, 115005 (2010)
34. D. Hooper et al., Phys. Rev. D **82**, 123509 (2010)
35. D.G. Cerdeno, O. Seto, J. Cosmol. Astropart. Phys. **0908**, 032 (2009)
36. D.G. Cerdeno, C. Munoz, O. Seto, Phys. Rev. D **79**, 023510 (2009)
37. D.G. Cerdeno et al., J. Cosmol. Astropart. Phys. **0706**, 008 (2007)
38. J.F. Gunion et al., arXiv:1009.2555
39. A.V. Belikov et al., Phys. Lett. B **705**, 82 (2011)
40. C. Arina, F. Fornengo, J. High Energy Phys. **11**, 029 (2007)
41. G. Belanger et al., J. High Energy Phys. **1107**, 083 (2011)
42. S. Chang et al., Phys. Rev. D **79**, 043513 (2009)
43. S. Chang et al., Phys. Rev. Lett. **106**, 011301 (2011)
44. R. Foot, Phys. Rev. D **81**, 087302 (2010)
45. R. Foot, Phys. Lett. B **703**, 7 (2011)
46. R. Foot, Phys. Rev. D **82**, 095001 (2010)
47. Y. Mambrini, J. Cosmol. Astropart. Phys. **1107**, 009 (2011)
48. Y. Mambrini, J. Cosmol. Astropart. Phys. **1009**, 022 (2010)
49. Y. Bai, P.J. Fox, J. High Energy Phys. **0911**, 052 (2009)
50. J. Alwall et al., Phys. Rev. D **81**, 114027 (2010)
51. M.Yu. Khlopov et al., Int. J. Mod. Phys. D **19**, 1385 (2010)
52. S. Andreas et al., Phys. Rev. D **82**, 043522 (2010)
53. M.S. Boucenna, S. Profumo, Phys. Rev. D **84**, 055011 (2011)
54. P.W. Graham et al., Phys. Rev. D **82**, 063512 (2010)
55. B. Batell, M. Pospelov, A. Ritz, Phys. Rev. D **79**, 115019 (2009)
56. E. Del Nobile et al., Phys. Rev. D **84**, 027301 (2011)
57. J. Kopp et al., J. Cosmol. Astropart. Phys. **1002**, 014 (2010)
58. V. Barger et al., Phys. Rev. D **82**, 035019 (2010)
59. S. Chang et al., J. Cosmol. Astropart. Phys. **1008**, 018 (2010)
60. J.L. Feng et al., Phys. Lett. B **703**, 124 (2011)
61. M.T. Frandsen et al., Phys. Rev. D **84**, 041301 (2011)
62. Y.G. Kim, S. Shin, J. High Energy Phys. **0905**, 036 (2009)
63. S. Shin, in *PoS IDM2010* (2011), p. 094
64. M.R. Buckley, Phys. Lett. B **703**, 343 (2011)
65. N. Fornengo et al., Phys. Rev. D **84**, 115002 (2011)
66. P. Gondolo et al., Phys. Rev. D **85**, 035022 (2012)
67. E. Kuflik et al., Phys. Rev. D **81**, 111701 (2010)
68. C. Arina et al., J. Cosmol. Astropart. Phys. **1109**, 022 (2011)
69. M.R. Buckley et al., Phys. Lett. B **702**, 216 (2011)
70. A. Bottino et al., arXiv:1112.5666
71. P. Belli et al., Phys. Rev. D **84**, 055014 (2011)
72. A. Bottino et al., Phys. Rev. D **85**, 095013 (2012)
73. D.N. Spergel, Phys. Rev. D **37**, 1353 (1988)
74. M.J. Lehner et al., astro-ph/9905074
75. G.J. Alner et al., Nucl. Instrum. Methods A **555**, 173 (2005)
76. P. Belli et al., Nuovo Cimento C **15**, 475 (1992)
77. R. Bernabei et al., Eur. Phys. J. C **28**, 203 (2003)
78. N.J.C. Spooner et al., in *International Workshop IDM* (World Scientific, Singapore, 1997), p. 481

79. Y. Shimizu, M. Minowa, H. Sekiya, Y. Inoue, Nucl. Instrum. Methods A **496**, 347 (2003)
80. P. Belli et al., Nucl. Instrum. Methods A **626–627**, 31 (2011)
81. P. Belli et al., J. Phys. G **38**, 115107 (2011)
82. J.B. Birks, *The Theory and Practice of Scintillation Counting* (Pergamon, London, 1964)
83. P.H. Heckmann, Z. Phys. **157**, 10 (1959)
84. P.H. Heckmann et al., Z. Phys. **162**, 84 (1961)
85. W.F. Kienzle, A. Flammersfeld, Z. Phys. **165**, 1 (1961)
86. K. Tsukada, S. Kikuchi, Nucl. Instrum. Methods **17**, 286 (1962)
87. K. Tsukada et al., Nucl. Instrum. Methods **37**, 69 (1965)
88. F.J. Kratochwill, Z. Phys. **234**, 74 (1970)
89. F.D. Brooks, D.T. Jones, Nucl. Instrum. Methods **121**, 69 (1974)
90. V.I. Tretyak, Astropart. Phys. **33**, 40 (2010)
91. E. Gatti, F. De Martini, in *Nuclear Electronics*, vol. 2 (IAEA, Vienna, 1962), p. 265
92. F.A. Kroger, in *Some Aspects of the Luminescence in Solids* (Elsevier, Amsterdam, 1948), p. 109
93. B.C. Grabmaier, IEEE Trans. Nucl. Sci. **NS-31**, 372 (1984)
94. Y.C. Zhu et al., Nucl. Instrum. Methods A **244**, 579 (1986)
95. F.A. Danevich et al., Prib. Tekh. Eksp. **5**, 80 (1989) [Instrum. Exp. Tech. **32**, 1059 (1989)]
96. L.L. Nagornaya et al., IEEE Trans. Nucl. Sci. **55**, 1469 (2008)
97. L.L. Nagornaya et al., IEEE Trans. Nucl. Sci. **56**, 994 (2009)
98. E.N. Galashov et al., Funct. Mater. **16**, 63 (2009)
99. F.A. Danevich et al., Nucl. Instrum. Methods A **544**, 553 (2005)
100. P. Belli et al., Phys. Lett. B **658**, 193 (2008)
101. P. Belli et al., Nucl. Phys. A **826**, 256 (2009)
102. I. Bavykina et al., IEEE Trans. Nucl. Sci. **55**, 1449 (2008)
103. F.A. Danevich et al., Phys. Rev. C **67**, 014310 (2003)
104. R. Bernabei et al., J. Instrum. **7**, P03009 (2012)
105. I. Holl et al., IEEE Trans. Nucl. Sci. **NS-35**, 105 (1988)
106. H. Kraus et al., Nucl. Instrum. Methods A **600**, 594 (2009)
107. R. Bernabey et al., Metallofiz. Noveishie Tekhnol. **30**, 477 (2008)
108. P. Belli et al., Nucl. Instrum. Methods A **615**, 301 (2010)
109. G.P. Kovtun et al., Funct. Mater. **18**, 121 (2011)
110. D.V. Poda et al., $CdWO_4$ crystal scintillators from enriched isotopes for double beta decay experiments. in *Rad. Meas. as a Proc. of LUMDETR-2012 Conference* (in press)
111. A.S. Barabash et al., J. Instrum. **06**, P08011 (2011)
112. R. Bernabei et al., Nucl. Instrum. Methods A **592**, 297 (2008)
113. P. Belli et al., Phys. Rev. D **84**, 055014 (2011)
114. R. Bernabei et al., Eur. Phys. J. C **53**, 205 (2008)